

FIRST INDUCED PLASTID GENOME MUTATIONS IN AN ALGA WITH SECONDARY PLASTIDS: *psbA* MUTATIONS IN THE DIATOM *PHAEODACTYLUM TRICORNUTUM* (BACILLARIOPHYCEAE) REVEAL CONSEQUENCES ON THE REGULATION OF PHOTOSYNTHESIS¹

Arne C. Materna^{3,5}, Sabine Sturm⁵, Peter G. Kroth, and Johann Lavaud^{2,4}

Group of Plant Ecophysiology, Biology Department, Mailbox M611, University of Konstanz, Universitätsstraße 10, 78457 Konstanz, Germany

Diatoms play a crucial role in the biochemistry and ecology of most aquatic ecosystems, especially because of their high photosynthetic productivity. They often have to cope with a fluctuating light climate and a punctuated exposure to excess light, which can be harmful for photosynthesis. To gain insight into the regulation of photosynthesis in diatoms, we generated and studied mutants of the diatom *Phaeodactylum tricornutum* Bohlin carrying functionally altered versions of the plastidic *psbA* gene encoding the D1 protein of the PSII reaction center (PSII RC). All analyzed mutants feature an amino acid substitution in the vicinity of the Q_B-binding pocket of D1. We characterized the photosynthetic capacity of the mutants in comparison to wildtype cells, focusing on the way they regulate their photochemistry as a function of light intensity. The results show that the mutations resulted in constitutive changes of PSII electron transport rates. The extent of the impairment varies between mutants depending on the proximity of the mutation to the Q_B-binding pocket and/or to the non-heme iron within the PSII RC. The effects of the mutations described here for *P. tricornutum* are similar to effects in cyanobacteria and green microalgae, emphasizing the conservation of the D1 protein structure among photosynthetic organisms of different evolutionary origins.

Key index words: chlorophyll fluorescence; D1 protein; diatom; electron transport; herbicide; photosystem II; Q_B pocket

Abbreviations: DCMU, (3-(3, 4-dichlorophenyl)-1, 1-dimethylurea); LHC, light-harvesting complex; OEC, oxygen evolving complex; PAM, pulse amplitude modulation; PQ, plastoquinone; PSII

RC, photosystem II reaction center; Q_A and Q_B, quinone A and B; WT, wildtype

Diatoms (Heterokontophyta, Bacillariophyceae) are a major group of microalgae ubiquitous in all marine and freshwater ecosystems. With probably >10,000 species, their biodiversity is among the largest of photosynthetic organisms, just after the higher plants (Mann 1999). Diatoms are assumed to contribute to about 40% of the aquatic primary production (i.e., ~20% of the annual global production) and to play a central role in the biochemical cycles of silica (which is part of their cell wall) and nitrogen (Sarhou et al. 2005). Their productivity has contributed largely to the structure of contemporary aquatic ecosystems (Falkowski et al. 2004). In contrast to the supposed primary origin of red algae, green algae, and higher plants, diatoms originate from a secondary endosymbiotic event in which a nonphotosynthetic eukaryote probably engulfed a eukaryotic photosynthetic cell related to red algae and transformed it into a plastid (Keeling 2004). This peculiar evolution has led to complex cellular functions and metabolic regulations recently highlighted by the publication of the genome of two diatom species (Armbrust et al. 2004, Bowler et al. 2008), *Thalassiosira pseudonana* and *Phaeodactylum tricornutum*. The complex cellular functions include aspects of photosynthesis (Wilhelm et al. 2006), photoacclimation (Lavaud 2007), carbon and nitrogen metabolism (Allen et al. 2006, Kroth et al. 2008), and response to nutrient starvation (Allen et al. 2008).

As for most microalgae, the photosynthetic efficiency and productivity of diatoms strongly depend on the underwater light climate (MacIntyre et al. 2000). Planktonic as well as benthic diatoms tend to dominate ecosystems characterized by highly turbulent water bodies (coasts and estuaries) where they have to cope with an underwater light climate with high-frequency irradiance fluctuations coupled with large amplitudes. Depending on the rate of water mixing, diatoms can be exposed to punctual or chronic excess light, possibly generating stressful

¹Received 27 June 2008. Accepted 16 March 2009.

²Author for correspondence: e-mail johann.lavaud@univ-lr.fr.

³Present address: Alm Laboratory, Civil and Environmental Engineering, Massachusetts Institute of Technology (MIT), 77 Massachusetts Ave., 48-208, Cambridge, MA 02139, USA.

⁴Present address: UMR CNRS 6250 'LIENSs', Institute for Coastal and Environmental Research, University of La Rochelle, 2 rue Olympe de Gouges, 17042 La Rochelle Cedex, France.

⁵These authors contributed equally to this work.

conditions that impair photosynthesis (i.e., photoinactivation/-inhibition) (Long et al. 1994, Lavaud 2007). In higher plants and cyanobacteria, the processes of PSII RC photoinactivation/-inhibition are strongly influenced by the redox state of the acceptor side of PSII with quinones (Q_A and Q_B) as primary electron acceptor (Vass et al. 1992, Fufezan et al. 2007).

Here we report on the generation and characterization of four *psbA* mutants of *P. tricornutum*. All mutants feature distinct amino acid exchanges in the D1 protein of PSII close to or within the Q_B -binding pocket. The point mutations resulted in a constitutive impairment of the PSII electron transfer in all mutants to different extents. To our knowledge, this is the first report of plastid genome mutants in an alga with secondary plastids.

MATERIALS AND METHODS

Strains and media used for producing the psbA mutants of P. tricornutum. *P. tricornutum* (University of Texas Culture Collection, strain 646) was grown at 22°C under continuous illumination at 50 $\mu\text{mol photons} \cdot \text{m}^{-2} \cdot \text{s}^{-1}$ in Provasoli's enriched F/2 seawater medium (Guillard and Ryther 1962) using 'Tropic Marin' artificial seawater at a final concentration of 50%, compared to natural seawater. When used, solid media contained 1.2% Bacto Agar (Difco Lab., Becton Dickinson and Co., Sparks, MD, USA).

Generation of psbA mutants from P. tricornutum. Construction of plasmid transformation vectors: Four transformation vectors were constructed harboring a 795 bp *psbA* fragment containing the Q_B -binding pocket. The *psbA* inserts of each vector carried individual point mutations leading to different substitutions of the amino acid serine encoded by the *PsbA* (D1) codon 264 (for details and a vector map, see Fig. S1 in the supplementary material). In addition to the nonsynonymous point mutations in codon 264, a second, silent point mutation was introduced into codon 268 (TCT to TCA, nt position 804) without changing the encoded amino acid. The purpose of the second point mutation was to delete a *BssSI* restriction site, thus allowing easy RFLP screening of putative transformants.

Biolistic transformation of P. tricornutum: Transformation of *P. tricornutum* was performed using a Bio Rad Biolistic PDS-1000/He Particle Delivery System (Bio-Rad, Hercules, CA, USA) as described previously (Kroth 2007). Gold particles with a diameter of 0.1 μm served as microcarriers for the DNA constructs. Bombarded cells were allowed to recover for 24 h before being suspended in 1 mL of sterile F/2 50% medium. Transformants (250 μL) were selected at 21°C under constant illumination (35 $\mu\text{mol photons} \cdot \text{m}^{-2} \cdot \text{s}^{-1}$) on agar plates containing 5 10^{-6} M DCMU herbicide (3-(3, 4-dichlorophenyl)-1,1-dimethylurea) and repeatedly streaked on fresh solid selective medium to obtain full segregation of the mutation.

Isolation of DNA and sequencing of wildtype and mutant psbA genes. Total nucleic acids from the wildtype (WT) and mutant cells were isolated via a cetyltrimethylammoniumbromide (CTAB)-based method (Doyle and Doyle 1990). Prior to the mutagenesis of *P. tricornutum*, the WT *psbA* gene and the surrounding genes were sequenced (NCBI accession no. AY864816) via primer walking (GATC, Konstanz, Germany). For the molecular characterization of mutants, a 795 bp fragment of the *psbA* gene was amplified as described in Figure S1, and both strands were fully sequenced (GATC, Konstanz, Germany).

Cell cultivation and preparation for physiological measurements. *P. tricornutum* WT and mutant cells were grown in 200 mL sterile F/2 50% medium (Guillard and Ryther 1962) at 21°C in airlift columns continuously flushed with sterile air. The cultures were illuminated at a light intensity of 50 $\mu\text{mol photons} \cdot \text{m}^{-2} \cdot \text{s}^{-1}$ with white fluorescent tubes (L58W/25, Universal white, OSRAM GmbH, Munich, Germany) with a 16:8 light:dark (L:D) cycle. Cells were harvested during the exponential phase of growth, centrifuged (Allegra 25R; Beckman Coulter GmbH, Krefeld, Germany) at 3,000g for 10 min, and resuspended in their culture medium to a final chl *a* concentration of 10 $\mu\text{g chl a} \cdot \text{mL}^{-1}$. The algae were continuously stirred at 21°C under low continuous light. For oxygen (O_2), chl fluorescence, and thermoluminescence measurements, cells were dark-adapted 20 min prior to measurement.

Protein extraction and Western blot analysis. Cells were harvested during the exponential phase of growth as described above and subsequently grinded in liquid nitrogen. The homogenized cells were resuspended in preheated (60°C) extraction buffer (125 mM Tris/HCl [pH 6.8], 4% [w/v] SDS, 200 μM PMSF, and 100 mM DTT) and, after heat treatment, extracted with acetone. After wash steps, the dried protein pellet was finally resuspended in extraction buffer. Total protein was separated by SDS-PAGE. Proteins were transferred electrophoretically onto a PVDF membrane (HybondTM-P, Amersham Biosciences UK Limited, Buckinghamshire, UK) and incubated with an antiserum against D1 (Anti-PsbA global antibody, AS05 084, Agrisera, Sweden). Detection was performed using the chemoluminescence detection system from Roche Diagnostics (BM Chemiluminescence Blotting Substrate POD; Roche Diagnostics GmbH, Mannheim, Germany).

Pigment extraction and analysis. Chl *a* amount was determined by spectrophotometry using the 90% acetone extraction method. For pigment extraction, cells were deposited on a filter and frozen in liquid nitrogen. Pigments were extracted with a methanol:acetone (70:30, v/v) solution. Pigment analysis was performed via HPLC as previously described (Lavaud et al. 2003). Cell counts were performed using a Thoma hemacytometer (LaborOptik, Friedrichsdorf, Germany).

Spectroscopy and PSI reaction center (P_{700}) concentration. The absorption spectra were obtained at room temperature with a DW-2 Aminco (American Instrument Co., Jessup, MD, USA) spectrophotometer, half-bandwidth 3 nm, speed 2 $\text{nm} \cdot \text{s}^{-1}$, OD = 0 at 750 nm, 50% F/2 medium as a reference. P_{700} quantity relative to chl *a* was determined as described earlier (Lavaud et al. 2002a) with the DW-2 Aminco spectrophotometer in dual beam mode (reference at 730 nm).

Thermoluminescence. Thermoluminescence patterns were measured with a self-made thermoluminometer following the procedure previously described (Gilbert et al. 2004). Flashes were single turn-over with duration of 25 μs . Samples were adjusted to 20 $\mu\text{g chl a} \cdot \text{mL}^{-1}$ for measurement.

Oxygen (O_2) concentration and photosynthetic light-response (P/E) curves. O_2 concentration was measured with a DW1-Clark electrode (Hansatech Ltd., Norfolk, UK) at 21°C. White light of adjustable intensity (measured with a PAR-sensor, LI-185A; Li-Cor Inc., Lincoln, NE, USA) was provided by a KL-1500 quartz iodine lamp (Schott, Mainz, Germany). Cell culture samples were dark-acclimated for 20 min before measurement. P/E curves were obtained by illuminating a 2 mL sample during 5 min at various light intensities. A new sample was used for each measurement. E_K , the irradiance for saturation of photosynthetic O_2 emission was estimated from P/E curves.

Chl fluorescence induction kinetics and DCMU resistance. Chl *a* fluorescence induction kinetics were performed with two instruments: a PEA-fluorometer (Walz, Effeltrich, Germany) for short-time kinetics (up to 200 ms), which allowed a classic

OJIP analysis (see Fig. S4 in the supplementary materials for details), and a self-made “continuous light” fluorometer (Parésys et al. 2005) for long-time kinetics (up to 100 s). Cells were adjusted to a concentration of $5 \mu\text{g chl } a \cdot \text{mL}^{-1}$ and $20 \mu\text{g chl } a \cdot \text{L}^{-1}$ for the PEA- and the self-made fluorometers, respectively.

DCMU resistance was evaluated measuring the inhibition of the PSII activity versus increasing DCMU concentrations (see Fig. S4 for details). The kill curves with DCMU and atrazine were performed by growing the cells on solid medium with increasing concentrations of herbicides; growth conditions were the same as described before.

Chl fluorescence yield. Chl fluorescence yield was monitored with a modified PAM-101 fluorometer (Walz) as described previously (Lavaud et al. 2002a). For each experiment, 2 mL was used. Sodium bicarbonate was added at a concentration of 4 mM to prevent any limitation of the photosynthetic rate by carbon supply. When used, DCMU was incubated with the cell suspension at the beginning of the dark-adaptation period. Fluorescence parameters were defined as described in Figure S4. The parameter used to estimate the fraction of reduced Q_A (Büchel and Wilhelm 1993) was $1 - qP$ where qP is the photochemical quenching of chl fluorescence. The rate of linear electron transport was calculated as follows:

$$\text{ETR} = \Phi\text{PSII} \times \text{PDF} \times \alpha \times 0.5 \quad (1)$$

where ΦPSII is the PSII quantum yield for photochemistry, PDF is the irradiance, and α is the PSII antenna size (equivalent to $1/I_{1/2}$ of Y_{SS} , see below).

Oxygen (O_2) yield per flash. The relative O_2 yield produced per flash during a sequence of single-turnover saturating flashes (O_2 sequence) was measured polarographically at 21°C with a flash electrode as described by Lavaud et al. (2002b). The flashes were separated by 500 ms allowing the reopening of PSII RCs by reoxidation of Q_A^- between each flash. The procedures used to record and calculate the steady-state O_2 yield per flash (Y_{SS} , an evaluation of the number of O_2 producing PSII RCs relative to chl a), the reciprocal of the half-saturating flash intensity of flash O_2 -evolution saturation curves ($1/I_{1/2}$ of Y_{SS} , an evaluation of the PSII antenna size), and the miss probability per PSII were the ones described in Figure S4.

RESULTS

Generating the P. tricornutum psbA mutants. In an attempt to establish stable plastid transformation in *P. tricornutum*, we aimed for allele replacement via homologous recombination. To minimize impact on the diatom, we decided to substitute the WT *psbA* gene with slightly modified versions carrying alternative point mutations in codon 264 (Fig. S2B, green boxes, in the supplementary material). These mutations lead to single amino acid substitutions that were previously reported to induce herbicide resistance and a reduction in the electron transport within the PSII RC (Ohad and Hirshberg 1992, Oettmeier 1999). Sequencing of the target region in several putative transformants revealed a variety of nonsynonymous (and in some cases additional synonymous) point mutations. In all experiments, the observed point mutations occurred apparently random and independently of the respective vector sequence. None of the obtained resistant strains carried the

same pair of point mutations that was supposed to be introduced into *psbA* by the utilized transformation vector (data not shown). Negative control experiments involving exclusive selection without preceding transformation, and biolistic transformation without vector DNA failed to generate resistant colonies. We sequenced 1,000 bp regions surrounding the Q_B pocket as well as coding and noncoding areas more distant to the *psbA* locus without finding other mutations than the ones described here. Yet, we cannot exclude the possibility that additional mutations have occurred at unknown loci. However, due to the selection on DCMU, which specifically interacts with the Q_B pocket of the D1 protein, additional mutations at other loci are likely to be detrimental and therefore selected against.

Although intriguing, this study is not focusing on the underlying molecular mechanism leading to the elevated mutation rates in the *psbA* gene; it will be the focus of a subsequent work. Instead, we characterized and compared in four selected mutants the physiological effects of different amino acid substitutions in the D1 protein of the PSII RC on the regulation of photosynthesis.

Localization of the mutations in the D1 protein and herbicide resistance of the P. tricornutum psbA mutants. The highly conserved D1 protein is part of the PSII RC in cyanobacteria and all phyla of plastid containing photosynthetic eukaryotes (Fig. S2A). The Q_B -binding pocket is located between the DE helix and the transmembrane E helix of the D1 protein (Kern and Renger 2007). The functional relevance of the Q_B -binding pocket (Fig. S2B) is highlighted by an amino acid sequence similarity of 97%–98% between pennate and centric diatoms, and a similarity of ~90%–93% between diatoms and members of the red lineage, the green lineage, and even cyanobacteria (Fig. S3 in the supplementary material). Sequencing the *psbA* genes of the four mutant strains revealed point mutations within or near the Q_B -binding pocket (Fig. S2B, red squares). The mutant V219I featured an amino acid exchange (Val to Ile at position 219) in transmembrane helix D. In mutant F255I, a Phe was changed to Ile in helix DE close to the Q_B pocket. S264A carries a Ser to Ala substitution within the Q_B pocket, and in L275W, Leu was changed to Trp in the helix E.

In comparison to the WT, the competitive binding of the herbicide DCMU to the Q_B pocket was altered to a different degree in all mutants (Fig. S4), among which S264A showed the highest resistance (3,000-fold). The level of resistance was confirmed by growth curves in the presence of increasing concentrations of DCMU (not shown). S264A was also highly resistant against the herbicide atrazine (500-fold).

Photosystem and light-harvesting properties, and growth of the P. tricornutum psbA mutants. At low light

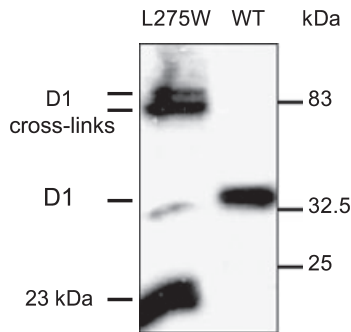


FIG. 1. Western blot of the D1 protein of the PSII reaction center of *Phaeodactylum tricornutum* wildtype (WT) and the *psbA* mutant L275W cells. Cells were grown at $50 \mu\text{mol photons} \cdot \text{m}^{-2} \cdot \text{s}^{-1}$. Bands representing D1 degradation products of 23 kDa and the cross-link products of ~ 83 kDa also resulting from D1 degradation (Ishikawa et al. 1999) were found in a larger amount in L275W but not in the WT.

intensity ($50 \mu\text{mol photons} \cdot \text{m}^{-2} \cdot \text{s}^{-1}$), the pigment contents of all the mutants and the WT cells were very similar, although the mutants tended to accumulate slightly more chl *a* per cell (see Fig. S4). The concentrations of active PSII RCs per chl *a*, Y_{SS} , and RC/CS_0 , were higher in all the mutants but L275W (Fig. S4). The low concentration for L275W was confirmed via Western blot analysis (Fig. 1). The molar PSI:PSII ratio was similar in WT and mutants with the exception of L275W, for which the ratio was higher ($\times 1.3$) ratio. The PSII LHC (light-harvesting complex) antenna size ($1/I_{1/2}$ of Y_{SS}) as well as E_{K} , the light intensity for saturation of photosynthesis, were lower in all the mutants, with the exception of V219I (Fig. S4).

We compared the physiological effects of the four mutations by measuring thermoluminescence, flash oxygen (O_2) yield emission (O_2 sequence), and chl *a* fluorescence induction kinetics. WT cells showed the expected thermoluminescence pattern with a strong B band (Fig. 2A) (Eisenstadt et al. 2008). While V219I showed the same pattern, in F255I and S264A the temperature of the maximal signal was shifted from 22°C to about 7°C and had significantly lowered amplitude (Fig. 2A). The O_2 sequences were highly damped in dark-adapted cells of F255I, S264A, and L275W (Fig. 2B) due to an increase in the miss probability (Fig. S4). In addition, in S264A and to a lesser extent in F255I (not shown), the O_2 production was increased at flash no. 2 (due to an increase of 10%–20% of the S_1 dark state in S264A compared to the WT), while in L275W, the maximum was at the flash no. 4 instead of no. 3. Chl *a* fluorescence induction kinetics are shown in Figure 2, C and D. All the mutants showed higher J ($\text{Q}_\text{A}^- \text{Q}_\text{B}^- / \text{Q}_\text{A}^- \text{Q}_\text{B}^{2-}$ state) and lower I ($\text{Q}_\text{A}^- \text{Q}_\text{B}^{2-}$ state) phases (Fig. 2C and Fig. S4), reflecting an impairment of the Q_A – Q_B electron transfer. The phenotype of V219I was the closest to WT phenotype, while F255I and L275W showed a significantly

higher J phase (+23% and 57%, respectively). S264A showed a drastically increased (by 71%) and delayed J phase and, in contrast to the other mutants, an increased I phase (see inset Fig. 2C and Fig. S4). When recorded over a longer timescale (100 s) and at continuous illumination, the pattern of the fluorescence induction kinetics of S264A and L275W was different (only L275W is shown, Fig. 2D). In S264A and L275W, the amplitude of the I-45 ms peak increased, and the whole pattern of the kinetics was disturbed.

The F_0 chl *a* fluorescence level was increased in all mutants (Fig. S4). Adding DCMU (resulting in inhibition of electron transport between Q_A and Q_B) to WT cells resulted in an increased F_0 (195 ± 6.5) comparable to S264A and L275W. When grown at low light intensity ($50 \mu\text{mol photons} \cdot \text{m}^{-2} \cdot \text{s}^{-1}$) all mutants showed a maximum photosynthetic efficiency of PSII (F_v/F_m , Fig. S4), which was similar to the WT cells, except for L275W (–19%). When measured at an equivalent irradiance, the effective PSII quantum yield (Φ_{PSII} , Fig. S4) was the same for WT cells and V219I, but lower in the other mutants. These values were in accordance with the steady-state electron transport rate per PSII (ET_0/CS_0 , Fig. S4). Addition of DCMU to the WT resulted in a decreased Φ_{PSII} (0.38), similar to that of S264A and L275W.

Only L275W showed a reduction in growth rate (–26% (μ , Fig. S4) and final maximal biomass (Fig. S5 in the supplementary material). Although F255I and S264A reached the same final biomass with the same growth rate as the WT, they showed a 24 h delay (see days 3 and 2, respectively, Fig. S5).

Photosynthetic capacity of the P. tricornutum psbA mutants as a function of the light intensity. The light intensity dependent impairment of the Q_A – Q_B electron transfer was evaluated by measuring $1 - \text{qP}$, a fluorescence parameter that estimates the fraction of reduced Q_A (Büchel and Wilhelm 1993). While $1 - \text{qP}$ was similar in WT and in V219I, it was the highest in S264A and L275W (Fig. 3A). A difference in the extent of Q_A reduction was also found at rather low light intensities (inset Fig. 3A) as indicated by the ratios of the extent of the I-45 ms peak from the long-time fluorescence induction kinetics of mutant versus WT (see Fig. 2D). In S264A and L275W, $1 - \text{qP}$ reached saturation earlier (between 250 and $400 \mu\text{mol photons} \cdot \text{m}^{-2} \cdot \text{s}^{-1}$) than in WT cells. In F255I, the extent of Q_A reduction was higher than in WT up to a light intensity of $400 \mu\text{mol photons} \cdot \text{m}^{-2} \cdot \text{s}^{-1}$. The direct consequences of the impaired Q_A – Q_B electron transfer were changed amplitudes of the electron transport rate per PSII (ETR) as well as altered patterns of ETR as a function of light intensity (Fig. 3B). The maximum ETR was decreased in all the mutants but to a different extent, thus confirming the values for ET_0/CS_0 (Fig. S4). In contrast to WT and the other mutants, ETR was already maximal in S264A and

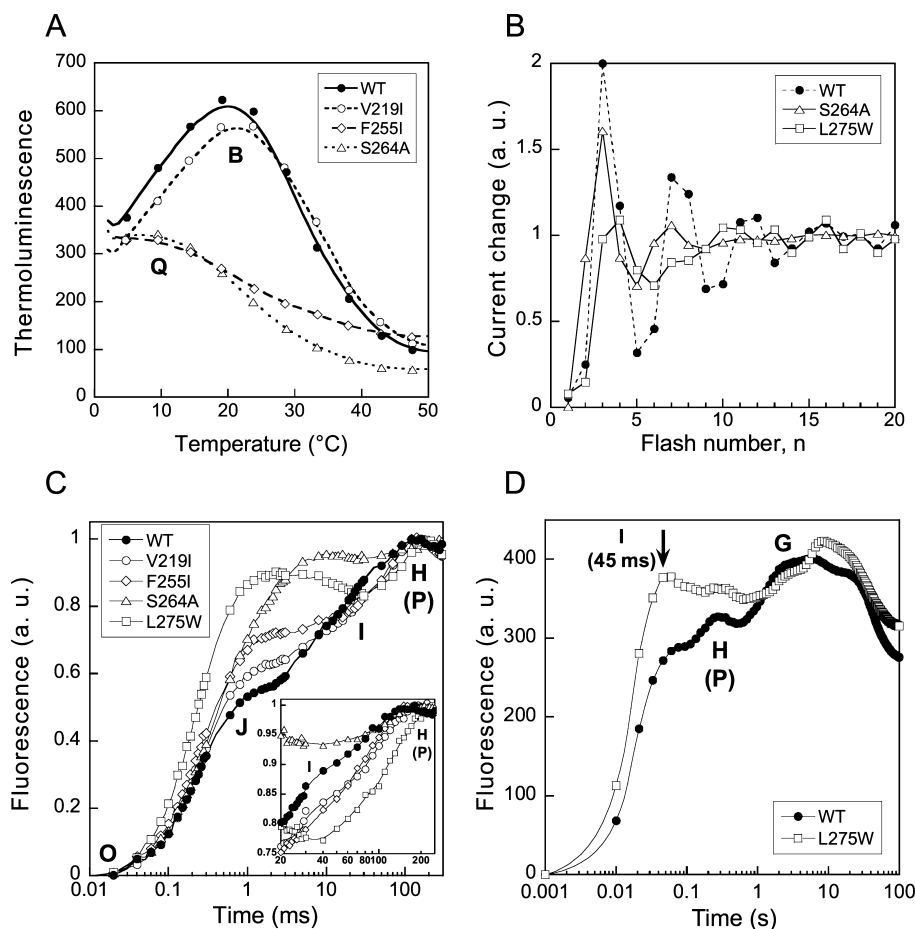


FIG. 2. (A) Thermoluminescence emission of dark-adapted cells of *Phaeodactylum tricornutum* wildtype (WT) and the *psbA* mutants V219I / F255I / S264A. The characteristic emission bands at 7°C (Q) and 22°C (B) are shown; they reflect the recombination states of the PSII reaction center $S_2Q_A^-$ and $S_2/3Q_B^-$ and the redox potential of Q_A and Q_B , and the redox potential of Q_A and Q_B , respectively (Gilbert et al. 2004, Eisenstadt et al. 2008). Curves represent the average of three measurements. (B) O₂ production in a series of single-turnover flashes (O₂ sequences) by dark-adapted cells of *P. tricornutum* WT and of the two *psbA* mutants S264A and L275W, as measured via a flash electrode. The pattern of the O₂ sequence for V219I resembled the one of the WT, and the pattern of F255I resembled the one of S264A with less pronounced features. See Figure S4 (in the supplementary material) for a detailed description. (C–D) Chl *a* fluorescence-induction kinetics reflect quantum yield changes of chl *a* fluorescence as a function of the illumination duration, which relates to both excitation trapping in PSII and the ensuing photosynthetic electron transport. (C) Short-time kinetics recorded via PEA fluorometer from dark-adapted cells of *P. tricornutum* WT and the four *psbA* mutants (V219I / F255I / S264A / L275W). The letters O, J, I, P, H, and G refer to the phases of the kinetics (Lazar 2006). (D) Long-time kinetics from dark-adapted cells of WT and L275W (same pattern for S264A) as recorded with a self-made “continuous light” fluorometer. The arrow indicates the first peak (I phase at 45 ms). The amplitude of I reflects the redox state of Q_A (Lavaud and Kroth 2006). In diatoms, the classic P peak is divided into two peaks, H and G (Lavaud and Kroth 2006, Lazar 2006).

L275W at a light intensity of 250 $\mu\text{mol photons} \cdot \text{m}^{-2} \cdot \text{s}^{-1}$; at this light intensity, the extent of Q_A reduction was close to its maximum (Fig. 3A).

DISCUSSION

Three out of the four *psbA* mutants showed a phenotype clearly distinct from the WT (see Fig. 4). Obviously, the observed amino acid substitutions hold implications for the phenotype of the mutants. The phenotypic effects described in this study allow various insights into the functionality of mutated residues or domains within the D1 protein.

A mutation that slightly affects the photosynthetic efficiency: V219I. In response to the slightly increased

reduction state of Q_A (+ 10%) and the decreased ETR per PSII (about 5%), in V219I the number of PSII RCs was increased (14% to 22%, depending on the method) to maintain a photosynthetic activity similar to the WT as reflected also by its growth pattern. Hence, the exchange of Val to Ile at the position 219 in the helix D appears to be too distant from the Q_B -binding pocket to significantly disturb the electron transport within the PSII RC in *P. tricornutum*.

Effects of mutations within the Q_B -binding pocket: F255I and S264A. The residues Phe₂₅₅ and Ser₂₆₄ bind the head group of Q_B (Kern and Renger 2007). The electron transport between Q_A and Q_B in F255I was significantly impaired (Fig. 4), slowing down the

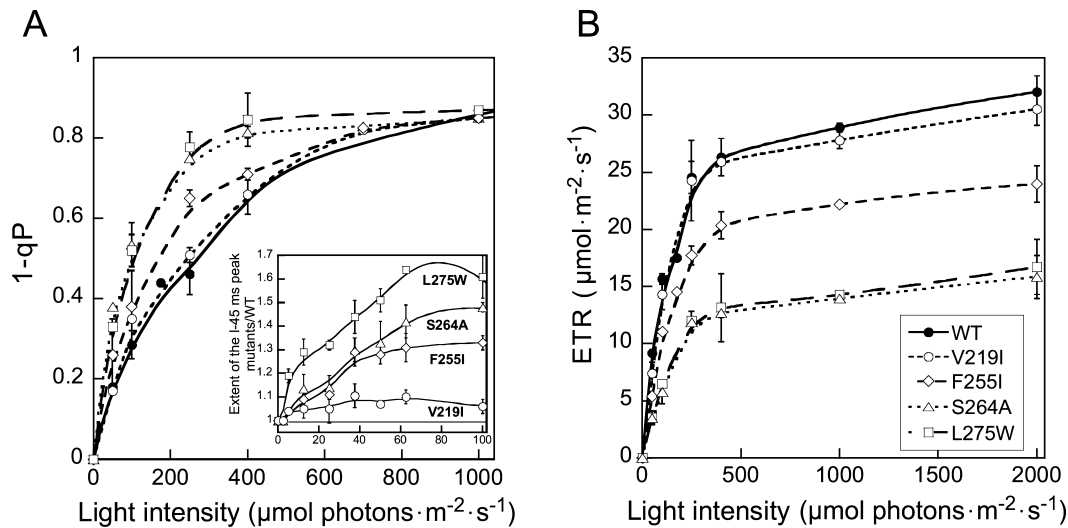


FIG. 3. Chl *a* fluorescence parameters as recorded with a PAM-fluorometer for the wildtype (WT) and the four *psbA* mutants (V219I / F255I / S264A / L275W) of *Phaeodactylum tricornutum* cells as a function of a light intensity gradient from darkness ($0 \mu\text{mol photons} \cdot \text{m}^{-2} \cdot \text{s}^{-1}$) to the equivalent of full sunlight in nature ($2,000 \mu\text{mol photons} \cdot \text{m}^{-2} \cdot \text{s}^{-1}$, Long et al. 1994). The illumination duration was 5 min; a new sample was used for each irradiance treatment. (A) $1 - qP$ estimates the fraction of reduced Q_A (Büchel and Wilhelm 1993). Inset: Ratio mutants versus WT of the amplitude of the I-45 ms peak (see Fig. 2D) up to $100 \mu\text{mol photons} \cdot \text{m}^{-2} \cdot \text{s}^{-1}$. (B) ETR is the rate of linear electron transport. See the Materials and Methods section and Figure S4 (in the supplementary materials) for details about the calculations of these parameters. Values are average \pm SD of three to four measurements.

reoxidation of Q_A^- as illustrated by the increased $Q_A Q_B^- / Q_A^- Q_B^-$ state. It was especially visible with the pattern of thermoluminescence that resembles the one reported in *P. tricornutum* for WT cells treated with DCMU (abolishment of the B band and increase of the Q band) (Eisenstadt et al. 2008). Backward electron transfer from Q_B^- to Q_A , as illustrated by an enhanced F_0 in photochemically inactive PSII RCs (Xiong et al. 1997), might partially explain the increased concentration of Q_A^- . As a consequence, the miss probability of the S state-cycle was increased, the S_1 state was stabilized (Perewoska et al. 1994), and the lifetimes of the redox states S_2 and S_3 increased (Gleiter et al. 1992), indicating a disturbed OEC operation. To compensate the decreased photochemistry of PSII, in F255I the number of PSII RCs increased (Fig. 4), reflected by a slight increase of chl *a* per cell as also reported for higher plants (Srivasatava et al. 1994). Nevertheless, the overall amount of pigments per chl *a* did not change; thus, the antenna size per PSII decreased, leading to a similar increase in E_K . Decreasing the PSII antenna size is known to be a straightforward way to relief from high excitation pressure on PSII due to a slowed down electron flow within the PSII RC because of mutations, herbicides, environmental stress, or other factors. Similarly, Wagner et al. (2006) suggested that in *P. tricornutum* an increased number of photosynthetic units together with decreased size of these units might allow maximization of photochemistry at different light regimes, which might be the case in mutants F255I and S264A. In spite of all these

changes, the potential for photochemistry, qP , was decreased at intermediary irradiances (up to $400 \mu\text{mol photons} \cdot \text{m}^{-2} \cdot \text{s}^{-1}$). At high light intensities, the ETR was reduced (Fig. 4), reflecting the decrease of the PSII antenna size and of Φ_{PSII} .

S264A showed a more drastic reaction compared to F255I regarding the Q_A^- reoxidation, the electron back transfer Q_B^- to Q_A , but also the Q_B^- / Q_B^{2-} reoxidation (increased $Q_A^- Q_B^{2-}$ state) (Fig. 4). Consequently, the operation of the OEC S-state cycle was strongly disturbed similar to the pattern of the fluorescence induction kinetics, illustrating the consequence of the modified Q_A-Q_B redox state on the whole electron transport chain and especially on the redox state of the plastoquinone (PQ) pool (Lazar 2006, Papageorgiou et al. 2007). As F255I, S264A reacted by increasing the PSII number. qP was largely diminished, which usually reflects accumulation of dysfunctional, highly reduced PSII RCs. It led to a decrease in ETR at all light intensities. Both qP and ETR were saturated at a much lower irradiance than in the WT. The exchange of Ser to Ala probably modified the spatial arrangement of the Q_B pocket (Gleiter et al. 1992, Perewoska et al. 1994), as illustrated by the high DCMU resistance, and greatly impaired not only the redox state of Q_B but the binding of Q_B itself (Della Chiesa et al. 1997).

Effects of a mutation close to the nonheme iron-binding site: L275W. Leu₂₇₅ is close to one of the histidines binding the nonheme iron atom (His₂₇₂ in helix E, grey bar in Fig. S2), as well as at nearly equal distance between Q_A and Q_B (Kern and Renger 2007).

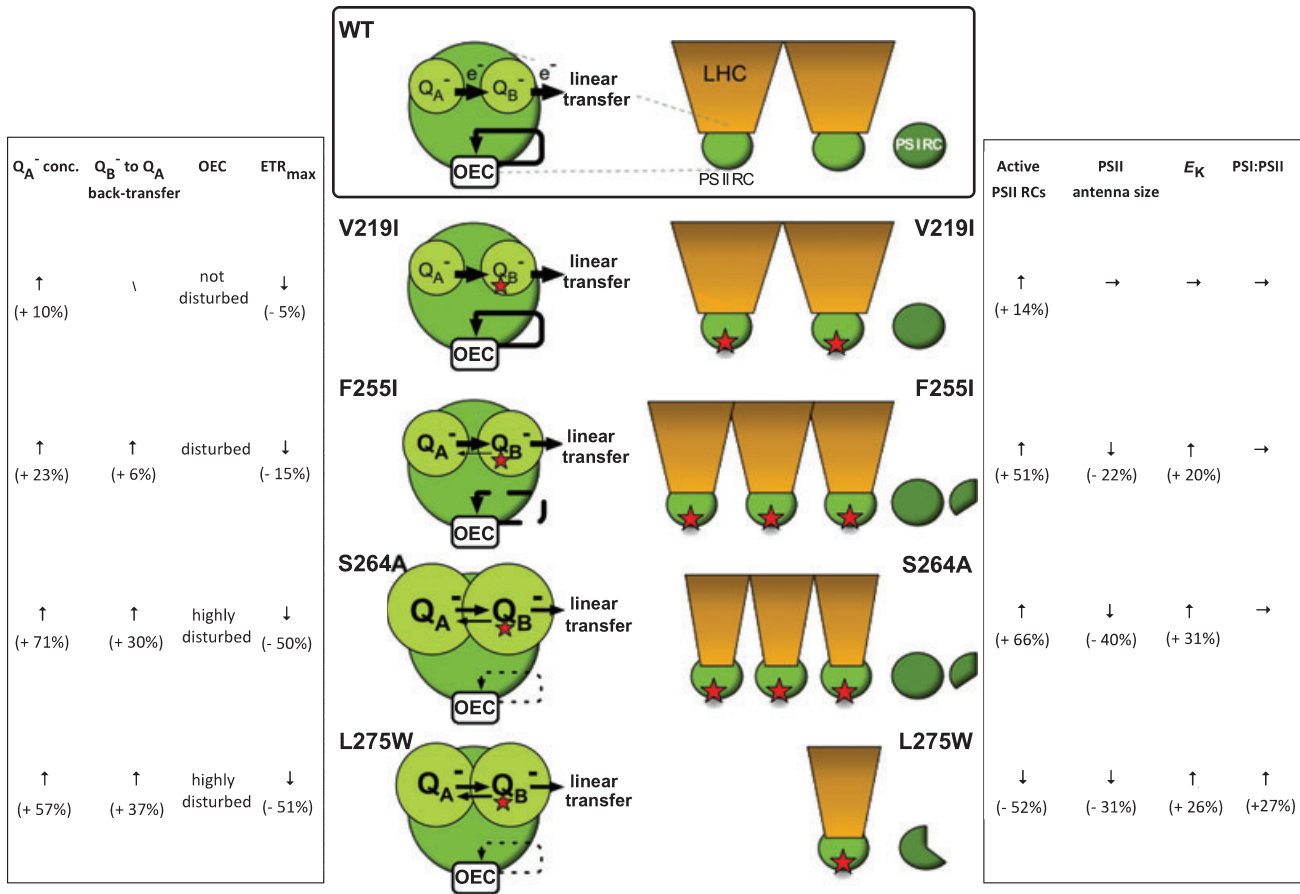


FIG. 4. Diagram of the influence of mutations on the photosynthetic apparatus of the *psbA* mutants (V219I/F255I/S264A/L275W) of *Phaeodactylum tricornutum* in comparison to the wildtype (WT) situation. Left: the electron pathways within the PSII reaction center; right: the architecture of the photosystems as a function of WT situation (PSI:PSII 1:2); arrow up: increased value (the true value is given in-between brackets); arrow down: decrease; flat arrow: no change. Symbols: red star, mutation; size of Q_A^-/Q_B^- , concentration of Q_A^-/Q_B^- ; thickness of the e^- arrows, value of the ETR_{max} and of the Q_B^- to Q_A back-transfer; dotted feature of the OEC arrow, proportion of the disturbance of the OEC operation. E_K , light intensity for saturation of photosynthesis; e^- , electrons; LHC, light-harvesting antenna complex; OEC, oxygen evolving complex; PSI/PSII RC, PSII/PSI reaction center; PSI:PSII, molar photosystem stoichiometry; Q_A and Q_B , quinones. See the text for a more detailed description.

The effect of the L275W mutation on the photosynthetic ability per PSII was similar to the point mutation S264A (Fig. 4) but showed a highly disturbed OEC operation along with increased Q_A reduction. Q_A reduction was already elevated (1.2- to 1.3-fold compared to WT) at light intensities that were even below the intensity used for growing the cells. Ultimately, L275W showed a decreased growth rate under low light as well as the inability to reach the same final maximal biomass. The main difference compared to the other mutants was the reduced amount of active PSII (Fig. 4), demonstrated by a disturbed D1 repair cycle. Mutations close to or within the Q_B pocket have been reported to modify the D1 turnover either by accelerating its damage and/or by inhibiting its proteolysis and/or synthesis (Della Chiesa et al. 1997, Nishiyama et al. 2006). Thus, it is very likely that in L275W there is a mixed population of active and inactive PSII, even at low light intensities (Mohanty et al. 2007), which is sup-

ported by the high F_0 level and the lowest F_v/F_m . In contrast to the other mutants, L275W responded to the point mutation by modifying the architecture of the photosynthetic apparatus as illustrated by the increase of the PSI:PSII stoichiometry (Fig. 4). This attempt to maintain a reasonable photosynthetic activity might lead to an increased capacity for PSI cyclic electron flow as in higher plants with deficient linear electron transport (Kotakis et al. 2006).

In a series of papers (reviewed in van Rensen et al. 1999), Govindjee et al. showed that the exchange of the residue Leu₂₇₅ significantly perturbs the Q_A -Fe- Q_B structure, the protonation of Q_B^{2-} (Xiong et al. 1997), and subsequently the PQ redox state. It is thus likely that the phenotype of L275W is due to the close vicinity of the point mutation to both the Q_B pocket and the nonheme iron atom binding sites, which functionally affects the properties of both the Q_A and Q_B pockets (Vermaas et al. 1994).

Effects of similar mutations in cyanobacteria and green algae. The effects of the mutations described here for the diatom *P. tricornutum* are similar to effects of the same mutations reported in other photosynthetic organisms. For example, it has also been concluded that in the green alga *Chlamydomonas reinhardtii* (Erickson et al. 1989), the V219I amino acid substitution does not significantly disturb the electron transport within the PSII RC. Also, the effects of the F255I, S264A, and L275W mutations have been described in cyanobacteria (*Synechocystis* and *Synechococcus*) and *C. reinhardtii* (Erickson et al. 1989, Etienne et al. 1990, Gleiter et al. 1992, Kless et al. 1994, Perewoska et al. 1994). Remarkably, the S264A-induced DCMU resistance was much higher in *P. tricornutum* than in all previously studied organisms (Gleiter et al. 1992).

CONCLUSION

Our results illustrate that not only the substitution loci but also the nature of the exchanged amino acids are essential in modifying the spatial arrangement and properties of the D1 protein (Kless and Vermaas 1994). Ultimately, such structural changes, especially in the Q_B-binding pocket, are defining the electron transport rate within the PSII RC (Lardans et al. 1998, Oettmeier 1999). The fact that photosynthesis is impaired at different levels in the *P. tricornutum psbA* mutants described here (see Fig. 4) provides a unique opportunity to further study the regulation of photosynthesis in diatoms.

This work was supported by the European network MarGenes (QLRT-2001-01226 to P. G. K.), the University of Konstanz (University of Konstanz, 'Anreizsystem zur Frauenförderung' to S. S. and J. L.), and the DFG (grant LA2368/2-1 to J. L.). We thank I. Adamska (University of Konstanz), C. Bowler (ENS Paris), and C. Wilhelm (University of Leipzig) for access to some of the instruments used here and for helpful discussions; D. Ballert for technical assistance; V. Reiser and P. Huesgen (University of Konstanz), B. Rousseau (ENS Paris), T. Jakob, and H. Wagner (University of Leipzig) for help with some of the experiments. This work is part of the PhD project of A. C. M. and of the diploma work of S. S.

- Allen, A. E., LaRoche, J., Maheswari, U., Lommer, M., Schauer, N., Lopez, P. J., Finazzi, G., Fernie, A. R. & Bowler, C. 2008. Whole-cell response of the pennate diatom *Phaeodactylum tricornutum* to iron starvation. *Proc. Natl. Acad. Sci. U. S. A.* 105:10438–43.
- Allen, A. E., Vardi, A. & Bowler, C. 2006. An ecological and evolutionary context for integrated nitrogen metabolism and related signaling pathways in marine diatoms. *Curr. Opin. Plant Biol.* 9:264–73.
- Armbrust, E. V., Berges, J. A., Bowler, C., Green, B. R., Martinez, D., Putnam, N. H., Zhou, S., et al. 2004. The genome of the diatom *Thalassiosira pseudonana*: ecology, evolution and metabolism. *Science* 306:79–86.
- Bowler, C., Allen, A. E., Badger, J. H., Grimwood, J., Jabbari, K., Kuo, A., Maheswari, U., et al. 2008. The *Phaeodactylum* genome reveals the evolutionary history of diatom genomes. *Nature* 455:239–44.
- Büchel, C. & Wilhelm, C. 1993. *In vivo* analysis of slow chlorophyll fluorescence induction kinetics in algae: progress, problems and perspectives. *Photochem. Photobiol.* 58:137–48.
- Della Chiesa, M., Friso, G., Deak, Z., Vass, I., Barber, J. & Nixon, P. 1997. Reduced turnover of the D1 polypeptide and photoactivation of electron transfer in novel herbicide resistant mutants of *Synechocystis* sp. PCC 6803. *Eur. J. Biochem.* 248: 731–40.
- Doyle, J. J. & Doyle, J. L. 1990. A rapid total DNA preparation procedure for fresh plant tissue. *Focus* 12:13–5.
- Eisenstadt, D., Ohad, I., Keren, I. & Kaplan, A. 2008. Changes in the photosynthetic reaction center II in the diatom *Phaeodactylum tricornutum* result in non-photochemical fluorescence quenching. *Environ. Microbiol.* 10:1997–2007.
- Erickson, J. M., Pfister, K., Rahire, M., Togasaki, R. K., Mets, L. & Rochaix, J.-D. 1989. Molecular and biophysical analysis of herbicide-resistant mutants of *Chlamydomonas reinhardtii*: structure–function relationship of the photosystem II D1 polypeptide. *Plant Cell* 1:361–71.
- Etienne, A.-L., Ducruet, J.-M., Ajlani, G. & Vernotte, C. 1990. Comparative studies on electron transfer in photosystem II of herbicide-resistant mutants from different organisms. *Biochim. Biophys. Acta* 1015:435–40.
- Falkowski, P. G., Katz, M. E., Knoll, A. H., Quigg, A., Raven, J. A., Schofield, O. & Taylor, F. R. J. 2004. The evolution of modern phytoplankton. *Science* 305:354–60.
- Fufezan, C., Gross, C. M., Sjödin, M., Rutherford, A. W., Krieger-Liszka, A. & Kirilovsky, D. 2007. Influence of the redox potential of the primary quinone electron acceptor on photoinhibition in photosystem II. *J. Biol. Chem.* 282:12492–502.
- Gilbert, M., Wagner, H., Weingart, I., Nieber, K., Tauer, G., Bergmann, F., Fischer, H. & Wilhelm, C. 2004. A new type of thermoluminometer: a highly sensitive tool in applied photosynthesis research and plant stress physiology. *J. Plant Physiol.* 161:641–51.
- Gleiter, H. M., Ohad, N., Kolke, H., Hirschberg, J., Renger, G. & Inoue, Y. 1992. Thermoluminescence and flash-induced oxygen yield in herbicide resistant mutants of the D1 protein in *Synechococcus* PCC7942. *Biochim. Biophys. Acta* 1140:135–43.
- Guillard, R. R. R. & Ryther, J. H. 1962. Studies of marine planktonic diatoms. I. *C. nana* (Hustedt) and *D. confervacea* (Cleve) Gran. *Can. J. Microbiol.* 8:229–38.
- Ishikawa, Y., Nakatani, E., Henmi, T., Ferjani, A., Harada, Y., Tamura, N. & Yamamoto, Y. 1999. Turnover of the aggregates and cross-linked products of the D1 protein generated by acceptor-side photoinhibition of photosystem II. *Biochim. Biophys. Acta* 1413:147–58.
- Keeling, P. 2004. A brief history of plastids and their hosts. *Protist* 155:3–7.
- Kern, J. & Renger, G. 2007. Photosystem II: structure and mechanism of the water: plastoquinone oxidoreductase. *Photosynth. Res.* 94:183–202.
- Kless, H., Oren-Shamir, M., Malkin, S., McIntosh, L. & Edelman, M. 1994. The *D-E* region of the D1 protein is involved in multiple quinone and herbicide interactions in photosystem II. *Biochemistry* 33:10501–7.
- Kless, H. & Vermaas, W. 1994. Many combinations of amino acid sequences in a conserved region of the D1 protein satisfy photosystem II function. *J. Mol. Biol.* 246:120–31.
- Kotakis, C., Petropoulou, Y., Stamatakis, K., Yiotis, C. & Manetas, Y. 2006. Evidence for active cyclic electron flow in twig chlorenchyma in the presence of an extremely deficient linear electron transport activity. *Planta* 225:245–53.
- Kroth, P. G. 2007. Genetic transformation – a tool to study protein targeting in diatoms. In Van der Giezen, M. [Ed.] *Methods in Molecular Biology – Protein Targeting Protocols*. Humana Press, Totowa, New Jersey, pp. 257–68.
- Kroth, P. G., Chiovitti, A., Gruber, A., Martin-Jézéquel, V., Mock, T., Schnitzler Parker, M., Stanley, M. S., et al. 2008. A model for carbohydrate metabolism in the diatom *Phaeodactylum tricornutum* deduced from comparative whole genome analysis. *PLoS ONE* 3:e1426.

- Lardans, A., Förster, B., Prasil, O., Falkowski, P. G., Sobolev, V., Edelman, M., Osmond, C. B., Gillham, N. W. & Boynton, J. E. 1998. Biophysical, biochemical, and physiological characterization of *Chlamydomonas reinhardtii* mutants with amino acid substitutions at the Ala²⁵¹ residue in the D1 protein that result in varying levels of photosynthetic competence. *J. Biol. Chem.* 273:11062–91.
- Lavaud, J. 2007. Fast regulation of photosynthesis in diatoms: mechanisms, evolution and ecophysiology (a review). *Funct. Plant Sci. Biotech.* 1:267–87.
- Lavaud, J. & Kroth, P. 2006. In diatoms, the transthylakoid proton gradient regulates the photoprotective non-photochemical fluorescence quenching beyond its control on the xanthophyll cycle. *Plant Cell Physiol.* 47:1010–6.
- Lavaud, J., Rousseau, B. & Etienne, A.-L. 2003. Enrichment of the light-harvesting complex in diadinoxanthin and implications for the nonphotochemical quenching fluorescence quenching in diatoms. *Biochemistry U. S. A.* 42:5802–8.
- Lavaud, J., Rousseau, B., van Gorkom, H. & Etienne, A.-L. 2002a. Influence in the diadinoxanthin pool size on photoprotection in the marine planktonic diatom *Phaeodactylum tricorutum*. *Plant Physiol.* 129:1398–406.
- Lavaud, J., van Gorkom, H. & Etienne, A.-L. 2002b. Photosystem II electron transfer cycle and chlororespiration in planktonic diatoms. *Photosynth. Res.* 74:51–9.
- Lazar, D. 2006. The polyphasic chlorophyll *a* fluorescence rise measured under high intensity of exciting light. *Funct. Plant Biol.* 33:9–30.
- Long, S., Humphries, S. & Falkowski, P. 1994. Photoinhibition of photosynthesis in nature. *Annu. Rev. Plant Physiol. Plant Mol. Biol.* 45:633–62.
- MacIntyre, H. L., Kana, T. M. & Geider, R. J. 2000. The effect of water motion on short-term rates of photosynthesis by marine phytoplankton. *Trends Plant Sci.* 5:12–7.
- Mann, D. G. 1999. The species concept in diatoms. *Phycologia* 38:437–95.
- Mohanty, P., Allakhverdiev, S. I. & Murata, N. 2007. Application of low temperatures during photoinhibition allows characterization of individual steps in photodamage and the repair of photosystem II. *Photosynth. Res.* 94:217–24.
- Nishiyama, Y., Allakhverdiev, S. I. & Murata, N. 2006. A new paradigm for the action of reactive oxygen species in the photoinhibition of photosystem II. *Biochim. Biophys. Acta* 1757:742–9.
- Oettmeier, W. 1999. Herbicide resistance and supersensitivity in photosystem II. *Cell. Mol. Life Sci.* 55:1255–77.
- Ohad, N. & Hirschberg, J. 1992. Mutations in the D1 subunit of photosystem II distinguish between quinone and herbicide binding sites. *Plant Cell* 4:273–82.
- Papageorgiou, G. C., Tsimilli-Michael, M. & Stamatakis, K. 2007. The fast and slow kinetics of chlorophyll *a* fluorescence induction in plants, algae and cyanobacteria: a viewpoint. *Photosynth. Res.* 94:275–90.
- Parésys, G., Rigart, C., Rousseau, B., Wong, A. W. M., Fan, F., Barbier, J.-P. & Lavaud, J. 2005. Quantitative and qualitative evaluation of phytoplankton populations by trichromatic chlorophyll fluorescence excitation with special focus on cyanobacteria. *Water Res.* 39:911–21.
- Perewoska, I., Etienne, A.-L., Miranda, T. & Kirilovsky, D. 1994. S₁ destabilization and higher sensitivity to light in metribuzin-resistant mutants. *Plant Physiol.* 104:235–45.
- van Rensen, J. J. S., Xu, C. & Govindjee 1999. Role of bicarbonate in photosystem II, the water-plastoquinone oxido-reductase of plant photosynthesis. *Physiol. Plant.* 105:585–92.
- Sarthou, G., Timmermans, K. R., Blain, S. & Tréguer, P. 2005. Growth physiology and fate of diatoms in the ocean: a review. *J. Sea Res.* 53:25–41.
- Srivastava, A., Mohanty, P. & Bose, S. 1994. Alterations in the excitation energy distribution in *Synechococcus* PCC 7942 due to prolonged partial inhibition of photosystem II. Comparison between inhibition caused by (a) presence of PSII inhibitors, (b) mutation in the D1 polypeptide of PSII. *Biochim. Biophys. Acta* 1186:1–11.
- Vass, I., Styring, S., Hundal, T., Koivuniemi, A., Aro, E.-M. & Andersson, B. 1992. Reversible and irreversible intermediates during photoinhibition of photosystem II: stable reduced Q_A species promote chlorophyll triplet formation. *Proc. Natl. Acad. Sci. U. S. A.* 89:1408–12.
- Vermaas, W., Vass, I., Eggers, B. & Styring, S. 1994. Mutation of a putative ligand to the non-heme iron in photosystem II: implications for Q(A) reactivity, electron transfer, and herbicide binding. *Biochim. Biophys. Acta* 1184:263–72.
- Wagner, H., Jakob, T. & Wilhelm, C. 2006. Balancing the energy flow from captured light to biomass under fluctuating light conditions. *New Phytol.* 169:95–108.
- Wilhelm, C., Büchel, C., Fisahn, J., Goss, R., Jakob, T., LaRoche, J., Lavaud, J., et al. 2006. The regulation of carbon and nutrient assimilation in diatoms is significantly different from green algae. *Protist* 157:91–124.
- Xiong, J., Hutchison, R. S., Sayre, R. T. & Govindjee. 1997. Modification of the photosystem II acceptor side function in a D1 mutant (arginine-269-glycine) of *Chlamydomonas reinhardtii*. *Biochim. Biophys. Acta* 1322:60–76.

Supplementary Material

The following supplementary material is available for this article:

Figure S1. Construction of the pGEM-T D1 transformation vectors.

Figure S2. Multiple sequence alignments and phylogenetic reconstruction.

Figure S3. Pair-wise comparison chart of D1 (PsbA) amino acid similarities and distances.

Figure S4. Pigment composition (in mol · 100 mol⁻¹ chl *a*) and photosynthetic properties of the wildtype (WT) and the *psbA* mutants of *Phaeodactylum tricorutum*.

Figure S5. Growth curves of the wildtype (WT) and the four *psbA* mutants (V219I/F255I/S264A/L275W) of *Phaeodactylum tricorutum* cells.

This material is available as part of the online article.

Please note: Wiley-Blackwell are not responsible for the content or functionality of any supplementary materials supplied by the authors. Any queries (other than missing material) should be directed to the corresponding author for the article.